

# Direct link between cytokine activity and a catalytic site for macrophage migration inhibitory factor

Melissa Swope, Hong-Wei Sun,  
Paul R.Blake<sup>1</sup> and Elias Lolis<sup>2</sup>

Department of Pharmacology, Yale University School of Medicine,  
333 Cedar Street, New Haven, CT 06510 and <sup>1</sup>Institute for Chemistry,  
Bayer Corporation, Pharmaceutical Division, West Haven, CT 06516,  
USA

<sup>2</sup>Corresponding author  
e-mail: elias.lolis@yale.edu

**Macrophage migration inhibitory factor (MIF) is a secreted protein that activates macrophages, neutrophils and T cells, and is implicated in sepsis, adult respiratory distress syndrome and rheumatoid arthritis. The mechanism of MIF function, however, is unknown. The three-dimensional structure of MIF is unlike that of any other cytokine, but bears striking resemblance to three microbial enzymes, two of which possess an N-terminal proline that serves as a catalytic base. Human MIF also possesses an N-terminal proline (Pro-1) that is invariant among all known homologues. Multiple sequence alignment of these MIF homologues reveals additional invariant residues that span the entire polypeptide but are in close proximity to the N-terminal proline in the folded protein. We find that *p*-hydroxyphenylpyruvate, a catalytic substrate of MIF, binds to the N-terminal region and interacts with Pro-1. Mutation of Pro-1 to a glycine substantially reduces the catalytic and cytokine activity of MIF. We suggest that the underlying biological activity of MIF may be based on an enzymatic reaction. The identification of the active site should facilitate the development of structure-based inhibitors.**  
*Keywords:* cytokine/enzyme/macrophage migration inhibitory factor/NMR/protein structure

## Introduction

Cytokines elicit biological responses by activating specific cell surface receptors. Macrophage migration inhibitory factor (MIF) was initially identified as a secretion product of activated T cells and was one of the first cytokines to be discovered (Bloom and Bennett, 1966; David, 1966). MIF has a long association with delayed-type hypersensitivity reactions, but recent studies with the recombinant protein and its antibodies have identified additional biological functions (Bernhagen *et al.*, 1996). Glucocorticoids induce the secretion of MIF which acts to override glucocorticoid inhibition of cytokine (TNF- $\alpha$ , IL-1 $\beta$ , IL-6 and IL-8) production in macrophages and T cells (Calandra *et al.*, 1995). The activation of T cells by mitogenic or antigenic stimuli is also partly regulated by MIF (Bacher *et al.*, 1996). Glycosylation-inhibition factor (GIF), a cytokine that is involved in the regulation of IgE synthesis, has been found to have an identical sequence to MIF (Mikayama *et al.*,

1993). The pleiotropic *in vitro* activities on immune cells and involvement of MIF in the pathophysiology of a number of pro-inflammatory diseases are consistent with a role for MIF as a cytokine.

While MIF shares many similarities with cytokines, some dissimilarities have also been noted. MIF is pre-formed in cells and lacks a signal sequence, in contrast to most cytokines which are produced in response to stimuli and secreted using the signal sequence pathway. MIF is also different from cytokines in that it catalyzes chemical reactions. MIF converts D-2-carboxymethylester-2,3-dihydroindole-5,6-quinone to 5,6-dihydroxyindole-2-carboxymethyl ester. This non-physiological activity, which has been termed D-dopachrome tautomerase, was discovered fortuitously during the study of melanin biosynthesis (Rosengren *et al.*, 1996). In an attempt to identify natural ligands for MIF, the keto-enol isomerizations of *p*-hydroxyphenylpyruvate (HPP) and phenylpyruvate were discovered to be catalyzed by MIF (Rosengren *et al.*, 1997). The separate localization of these substrates from MIF as well as the kinetic parameters for the tautomerization reactions suggests that these molecules also are unlikely to be physiological substrates for MIF.

The three-dimensional structure of MIF is unlike that of any known cytokine. The MIF monomer possesses two antiparallel  $\alpha$ -helices that pack against a  $\beta$ -sheet in a motif that is somewhat reminiscent of MHC and dimeric  $\alpha$ -chemokines; however, the topology of MIF is totally different from these proteins. Three monomers associate to form a trimer in all of the crystal forms of MIF that have been characterized (Kato *et al.*, 1996; Sun *et al.*, 1996a; Suzuki *et al.*, 1996). Interestingly, MIF bears striking structural similarity to three microbial enzymes: 4-oxalocrotonate tautomerase (OT), 5-carboxymethyl-2-hydroxymuconate isomerase (CHMI), and chorismate mutase (Chook *et al.*, 1994; Subramanya *et al.*, 1996). These three enzymes are homotrimers (OT is a trimer of a homodimer) that possess active sites in close proximity to subunit interfaces. The similarity of MIF to OT and CHMI extends to at least one active site residue. OT and CHMI utilize an N-terminal proline as a catalytic base in their respective isomerization reactions (Whitman *et al.*, 1991; Hajipour *et al.*, 1993). MIF also possesses an N-terminal proline, the function of which has not been examined. We used sequence analysis, structural studies and mutational analysis to probe the function of Pro-1 and investigate the mechanism of MIF activity. Our studies correlate catalysis by MIF with neutrophil activation and suggest that an enzymatic reaction may underlie immune activation.

## Results

### **Sequence analysis identifies the potential biological site**

The significance of the unexpected structural and active site similarity of MIF with OT and CHMI was first

## A MIF Homologues

	*	**		**		*	***	*
Human MIF	<b>PMFIVNTNVP</b>	RASV.PDGFL	SELTQQLAQA	<b>TGKPPQYI</b> AV	HV.VPDQLMA	FGGSSEPCAL	CSLHSIGKIG	GA.QNRSYSK
Bovine MIF	<b>PMFVNTNVP</b>	RASV.PDGLL	SELTQQLAQA	<b>TGKPAQYI</b> AV	HV.VPDQLMT	FGGSSEPCAL	CSLHSIGKIG	GA.QNRSYSK
Rat MIF	<b>PMFIVNTNVP</b>	RASV.PEGFL	SELTQQLAQA	<b>TGKPAQYI</b> AV	HV.VPDQLMT	FRGTNDPCAL	CSLHSIGKIG	GA.QNRSYSK
Murine MIF	<b>PMFIVNTNVP</b>	RASV.PEGFL	SELTQQLAQA	<b>TGKPAQYI</b> AV	HV.VPDQLMT	FSGTNDPCAL	CSLHSIGKIG	GA.QNRSYSK
Chicken MIF	<b>PMFTIHTNVC</b>	KDAV.PDSLL	GELTQQLAKA	<b>TGKPAQYI</b> AV	HI.VPDQMMS	FGGSTDPICAL	CSLYSIGKIG	GQ.QNKTYTK
Human DT	<b>PFLELDTNLP</b>	ANRV.PAGLE	KRLCAAATAI	<b>LKGPADR</b> VNV	TVR.PGLAMA	LSGSTPCAQ	CSISSIGVVG	TARDNRSHSK
Rat DT	<b>PFVELETNLP</b>	ASRI.PAGLE	NRLCAATATI	<b>LKGPEDR</b> VSV	TIR.PGMTLL	MNKSTPCAQ	LLISSIGVVG	TAEQNRSHSA
Arab. MIF	<b>PCLNLTNVP</b>	LDGVTSSIL	SEASSTVAKI	<b>IGKPENY</b> VMI	.VLKGSVPMS	FGGTEPCAA	GELVSIAGLN	AD.VNKKLSS
C. el.MIF	<b>PMVRVATNLP</b>	NEKV.PVDPE	IRLTDLLARS	<b>MGKPRER</b> IAV	EIAAGARLV	HGATHDPVT	ISIKSIGAVS	AE.DNIRNTA
Bm MIF	<b>PYFTIDTNIP</b>	QNSI.SSAFL	KKASNVVAKA	<b>IGKPE</b> SYVSI	HVNVGGQAMV	FGGSEDPICAV	CVLKSIKCVG	PK.VNNSHAA
Wm MIF	<b>PYFTIDTNKP</b>	QDSI.SSAFL	KKAPNVVPKA	<b>.GKPE</b> SYVSI	HVN.GGQPMV	MGGSEDPICPV	CVLKSIKCVG	PK.VNNSHAE
Human MIF	LLCGLLAERL	RISPDRVYIN	YYDMNAANVG	WNNSTFA* . . .				
Bovine MIF	LLCGLLTERL	RISPDRYIIN	YCDMNAANVG	WNGSTFA. . .				
Rat MIF	LLCGLLSDRL	HISPDRVYIN	YYDMNAANVG	WNGSTFA* . . .				
Murine MIF	LLCGLLSDRL	HISPDRVYIN	YYDMNAANVG	WNGSTFA* . . .				
Chicken MIF	LLCDMIAKHL	HVSADRVYIN	YFDINAANVG	WNGSTFA* . . .				
Human DT	HFFEFLLTEL	ALGQDRILLR	FFPLESWQIG	KIGTMVTF . . .				
Rat DT	SFFKFLTEEL	SLDQDRILLR	FFPLESWQIG	KKGTVMTF . . .				
Arab. MIF	AVSAILETKL	SVPKSRFFLK	FYDTKGSFFG	WNGATL. . .				
C. el.MIF	AITFCGKEL	GLPKDKVVIT	FHDLPPATVG	FNGTTVAEA NKK				
Bm MIF	KLYKLLADEL	KIPKNRCYIE	FVDIEASSMA	FNGSTLLG. . .				
Wm MIF	KLYKLLADEL	KIPKNRCYIE	SVDIEASSMA	FNGSTFG. . . . .				

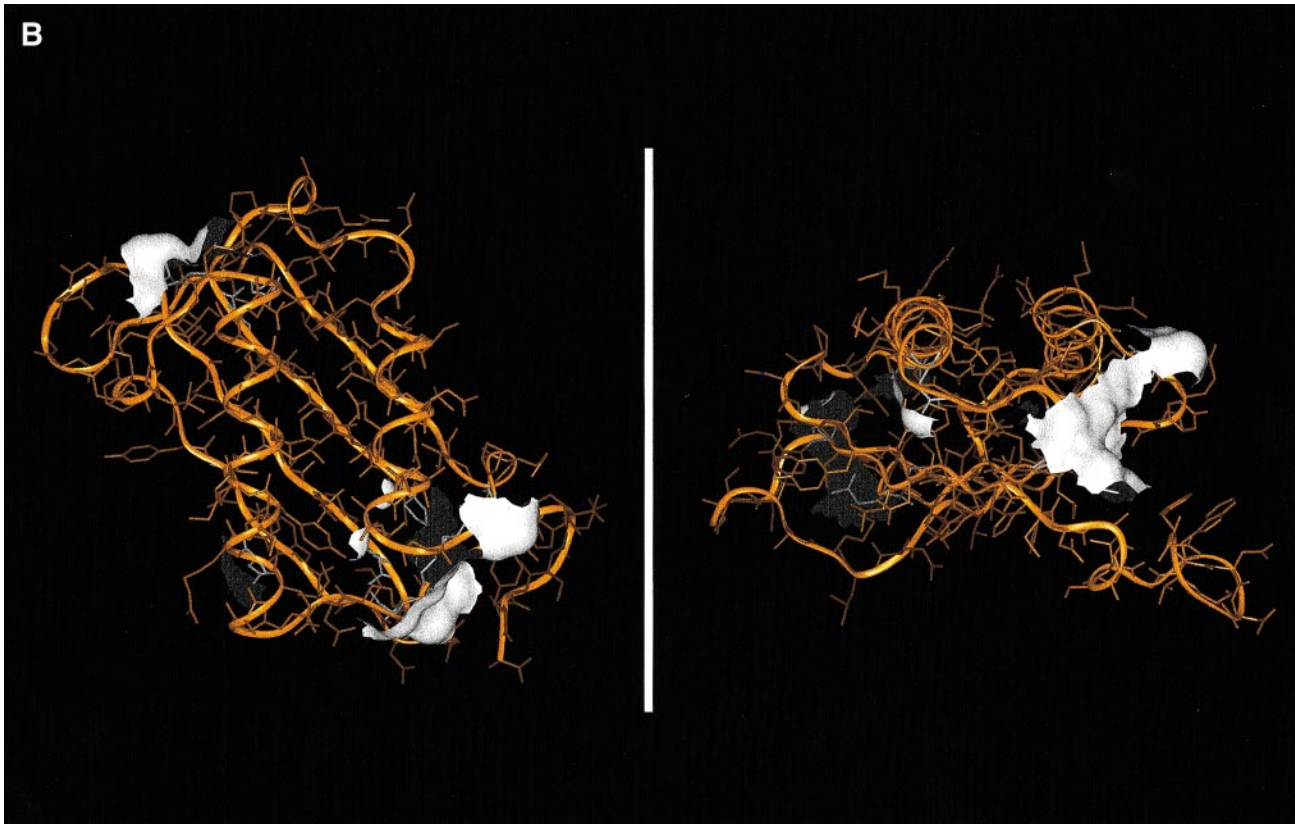


**Fig. 1.** (A) Multiple sequence alignment of all known homologues of MIF. Residues shown in bold with stars above them are invariant. DT, D-dopachrome tautomerase; Arab., *Arabidhopsis thaliana*; C. el., *Caenorhabditis elegans*; Bm, *Brugia malayi*; Wm, *Wuchereria bancrofti*. (B) Two views of the invariant residues (white) and their solvent-accessible surface area in the context of the ribbon structure of MIF. For clarity, only the monomer of MIF is shown. The two views are related by a 90° rotation.

investigated by sequence analysis. The sequence databases were searched with ENTREZ and BLAST to identify all MIF homologues. Pairwise identities among the 11 identified sequences range from 22 to 98%. Each of these sequences have a proline following the initiating methionine. Direct N-terminal sequencing of native MIF from two species (bovine and murine) reveals that the initiating methionine is removed in both cases, resulting in a protein with a proline at the N-terminus (Galat *et al.*,

1993; Bernhagen *et al.*, 1994). Due to the unique geometric restraints imposed by a proline, its prevalence at the N-terminus might be determined by the efficiency of removal of the initiating methionine in a Met-Pro sequence rather than by any functional requirement for an N-terminal proline. To investigate the statistical significance of proline at the N-terminus, the N-terminal residue of all proteins in the SWISSPROT database was analyzed. The majority (~80%) of proteins retain the initiating methionine. Of the

remaining proteins, proline is the fifth most prevalent amino acid at the N-terminus. If normalized by the number of codons for proline, the presence of a proline is slightly below average, but certainly not rare.

To investigate further the importance of the N-terminal region of MIF in its biological activity, multiple sequence alignment of the 11 MIF homologues was used for identifying additional invariant residues (Figure 1A). Only 11 residues (10% of the sequence) are invariant among all of the homologues, which represent a broad range of the evolutionary spectrum. These invariant residues can be expected to serve important functional or structural roles. Display of these residues on the three-dimensional structure of MIF shows that most of these residues cluster around the N-terminal proline and illustrate the evolutionary pressure to preserve this site (Figure 1B). Moreover, a solvent accessibility analysis reveals that many of these residues are exposed to solvent with the N-terminus sitting at the base of a pocket formed by the invariant residues. The clustering of invariant, solvent-exposed residues to form a pocket containing potential functional groups resembles an enzymatic active site.

#### **The N-terminus of MIF has an unusually low $pK_a$**

For the N-terminal amine of a protein to serve as a catalytic base, the  $pK_a$  of the amine must be at or below the physiological pH, otherwise the amine will be positively charged without a lone pair of electrons available for proton abstraction. Titration of proline amide indicates that the secondary amine of a proline has a  $pK_a > 9$  (Stivers *et al.*, 1996). To determine whether the  $pK_a$  of the N-terminus of MIF is consistent with a role as a catalytic base, the titration of Pro-1 was monitored directly by  $^{15}\text{N}$  NMR. The Pro-1  $^{15}\text{N}$  chemical shift appears between 43 and 52 p.p.m. and is well resolved from other  $^{15}\text{N}$  resonances of MIF in the pH range 4.4–8.5 (Figure 2A). At this pH range, MIF is folded as determined by circular dichroism and NMR measurements (data not shown). Non-linear least squares of the equation

$$\delta(\text{p.p.m.})^{\text{app}} = \frac{\delta_1 + \delta_2(10^{\text{pH}-pK_a})^n}{[(10^{\text{pH}-pK_a})^n + 1]}$$

where  $n$  is the Hill coefficient and  $\delta_1$  and  $\delta_2$  are the limiting chemical shifts at low and high pH, respectively, was used to determine a  $pK_a$  of  $5.6 \pm 0.1$  for Pro-1 (Figure 2B). This value is almost four pH units less than the  $pK_a$  of proline amide (Stivers *et al.*, 1996). The environment of Pro-1 was examined to determine the source of the unusual  $pK_a$ . The secondary amine of Pro-1 in the 1.9 Å X-ray structure of human MIF is at the base of a cleft surrounded predominantly by carbon atoms (not shown), suggesting that the low  $pK_a$  of the N-terminus is due to its location in a hydrophobic environment that lacks a neutralizing negative counter-charge. Calculation of an electrostatic potential map reveals an alternative explanation for the unusually low  $pK_a$ . A region of positive potential (Figure 3) is present at the N-terminus, with Lys66 and the invariant residue Lys32 providing the source of this positive potential. Determination of the relative contribution of the hydrophobic residues adjacent to the N-terminal proline versus the positive potential provided by Lys32 and Lys66 will require detailed biophysical

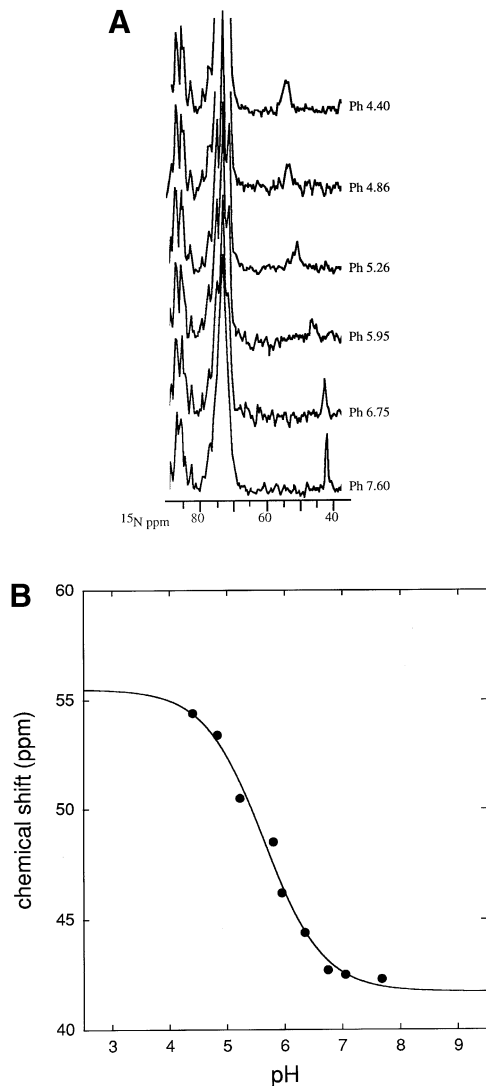


**Fig. 2.**  $pK_a$  determination of the N-terminal proline in human MIF using  $^{15}\text{N}$  NMR. (A) Stacked  $^{15}\text{N}$  NMR spectrum obtained for MIF at six pH values, ranging from 4.4 to 7.6. Data were acquired on  $^{15}\text{N}$ -labeled MIF (2.3 mM) with 25–90 k scans for each experiment. (B) Titration curve for the pH-dependent  $^{15}\text{N}$  chemical shift of the N-terminal proline. The curve was generated from a non-linear least-squares fit of the data and defines the  $pK_a$  of this proline to be  $5.6 \pm 0.1$ .

measurements and mutational analysis. Nonetheless, the environment at Pro-1 lowers the  $pK_a$  of the N-terminus such that the amine is unprotonated at physiological pH.

#### **The catalytic site**

The unusually low  $pK_a$  for the N-terminal amine, the presence of invariant residues at and around this site and the global structural similarity with two microbial enzymes led to the hypothesis that the N-terminal region may function as an active site. This hypothesis is consistent with the ability of MIF to catalyze isomerization reactions. While D-dopachrome (2-carboxy-2,3-dihydroindole-5,6-quinone), phenylpyruvate and HPP are unlikely to be the physiological substrates for a MIF-catalyzed reaction, these molecules provide suitable probes for examining whether the N-terminal region of MIF is involved in catalysis. Unfortunately, D-dopachrome is unstable for

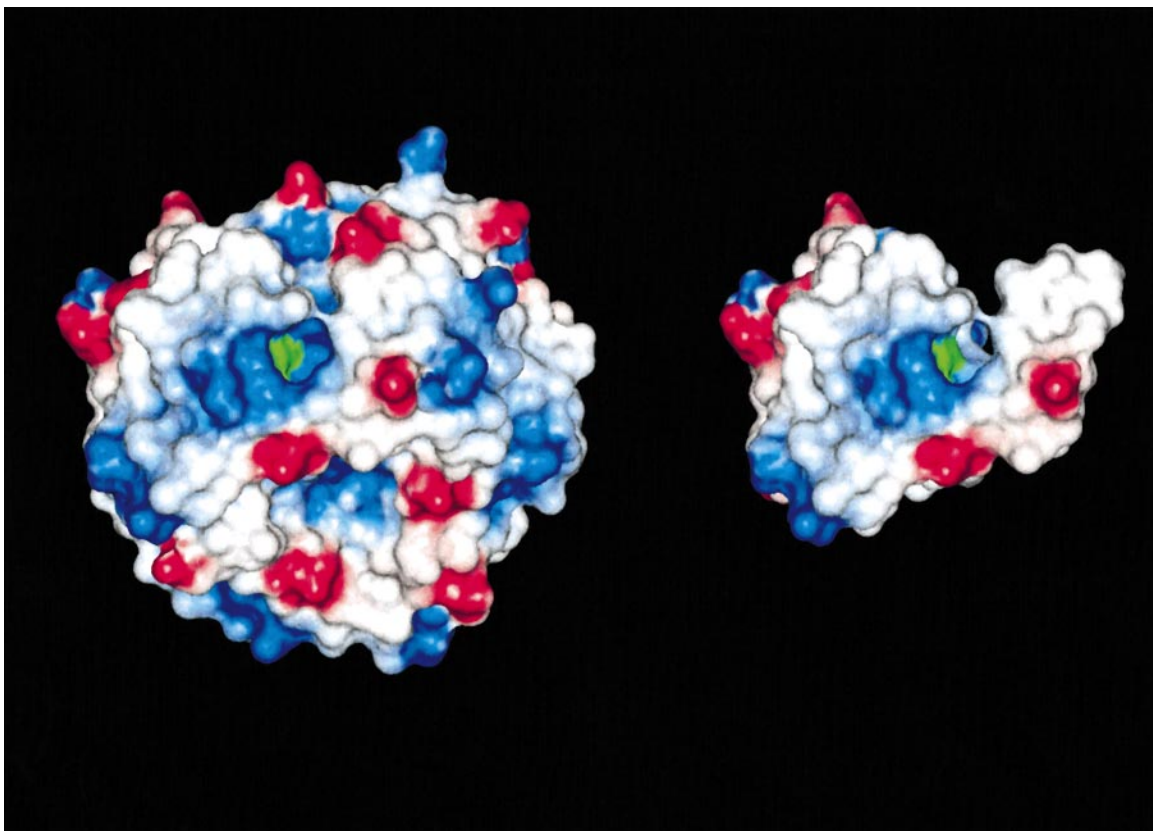


**Fig. 3.** Electrostatic potential map of the MIF trimer (left) and monomer (right). The map was calculated using DELPHI (MSI, San Diego, CA) with unit charges for the side chains of arginine, aspartic acid, glutamic acid and lysine, +0.5 charge for histidine side chains, and no charge for the terminal amine and carboxylate. The dielectric constant for the interior and exterior of the protein was 2 and 80, respectively. Negatively charged surfaces are in red, positively charged surfaces in blue. To distinguish the N-terminal proline from other residues, the color of its surface is changed from blue to green.

structural studies, and efforts to characterize crystallographically the interactions of phenylpyruvate or HPP have been unsuccessful due to the inability to obtain co-crystals. As these three substrates have been shown to compete with each other for binding to MIF, HPP was used to identify the active site using NMR spectroscopy. The initial experiment probed the chemical environment of the N-terminal amine in the presence of HPP. The  $^{15}\text{N}$  chemical shift of Pro-1 was measured as a function of varying concentrations of HPP. Figure 4A indicates that the peak shifts and broadens in the presence of 8 mM HPP (4 MIF equivalents) and disappears at 16 mM HPP. The severe broadening observed for this peak is suggestive of conformational exchange in the presence of HPP. This is at least partly due to the presence of both the keto and enol forms of HPP in the active site.  $^1\text{H}$ - $^{15}\text{N}$  HSQC spectra of MIF (Muhlhahn *et al.*, 1996) in the presence of HPP identify a much larger set of residues with changes in chemical shift. The resonance peaks for Ile4, Ala38 and Ile64 are not detectable in the  $^1\text{H}$ - $^{15}\text{N}$  HSQC spectrum at 10 mM HPP. Other residues with perturbed  $^1\text{H}$  or  $^{15}\text{N}$  chemical shifts include Phe3, Val39, Gly50, Lys66, Asn102, Gly107, Trp108, Phe113 and Ala114 (Figure 4B). While it is not possible to discriminate between chemical shifts that change due to ligand binding and those that are altered due to conformational changes, mapping of residues with chemical shifts greater than one standard deviation on the trimer of MIF illustrate that they cluster around

Pro-1 (Figure 4C). Moreover, these results provide evidence that the catalytically active form of MIF is defined by multiple subunits as two residues that cluster around Pro-1 arise from a different subunit.

#### **Correlation between neutrophil priming and catalytic activity**

To probe further the role of Pro-1 in the catalytic and biological activity of MIF, a single site-directed mutant was generated in which proline is substituted by glycine (P1G). The P1G mutant was expressed and purified as previously described for wild-type MIF (Sun *et al.*, 1996b). The folding of P1G as assessed by circular dichroism and  $^1\text{H}$  NMR spectra is identical to that of wild-type MIF (data not shown). However, P1G does not have any measurable catalytic activity with L-dopachrome methyl ester (a substrate similar to D-dopachrome) and HPP during the timescale of the assay and the concentrations tested (Figure 5A and B). Wild-type MIF displays a  $K_m$  of  $143 \pm 23 \mu\text{M}$  and  $1.3 \pm 0.45 \text{ mM}$  for each substrate, respectively.

To determine whether elimination of catalytic activity affected biological activity, a neutrophil priming assay measuring superoxide generation was used. Wild-type MIF displays an  $\text{ED}_{50}$  of  $8.6 \pm 3.3 \text{ ng/ml}$  ( $0.7 \pm 0.3 \text{ nM}$ ) in this assay with a maximal increase in superoxide production that ranges between 20 and 30% (Figure 6A). In contrast, superoxide secretion by P1G is significantly

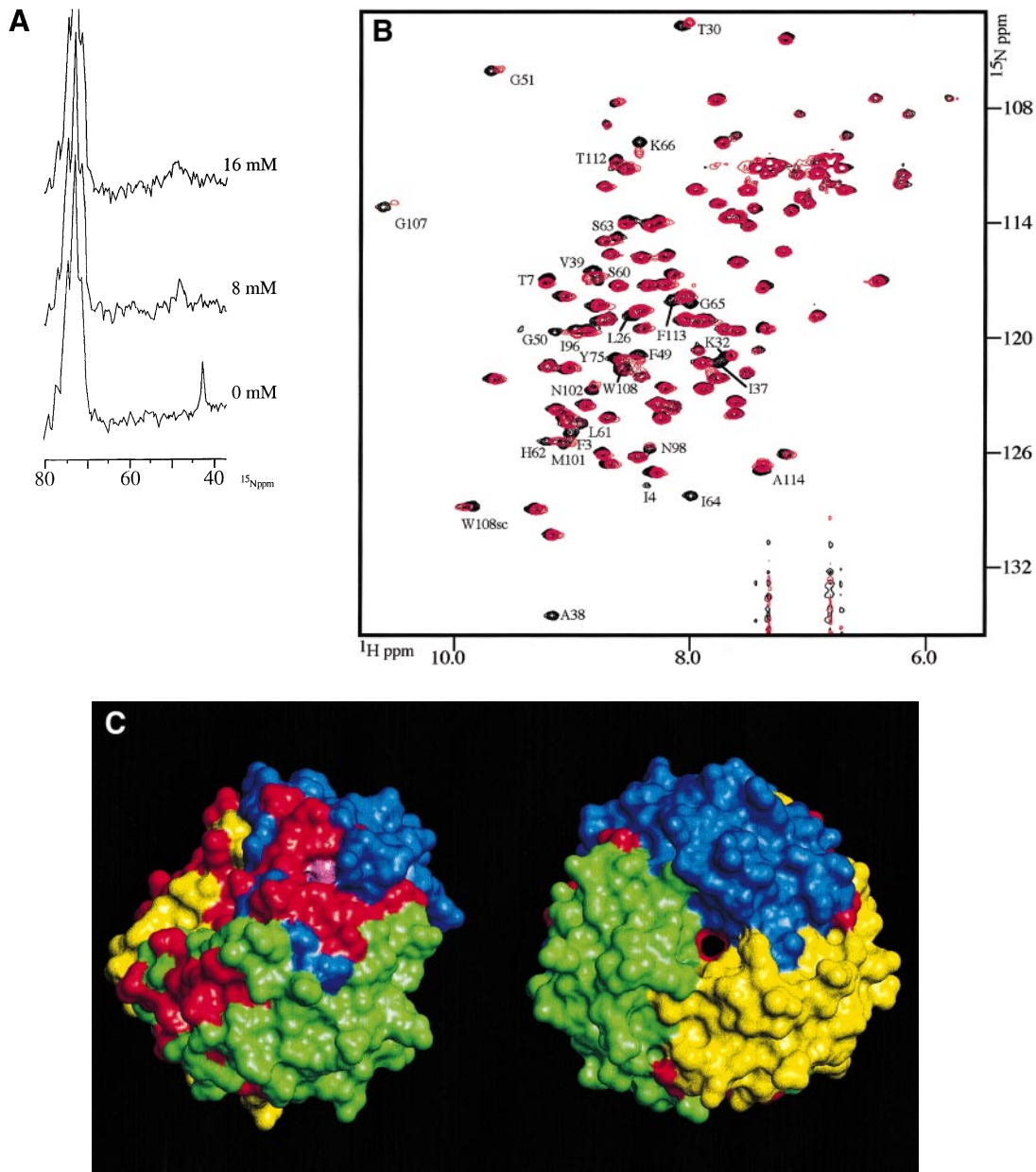


**Fig. 4.** (A)  $^{15}\text{N}$  NMR spectrum of Pro-1 in the presence of varying concentrations of HPP. The chemical shift and broadening effects observed indicate a perturbation in the electronic environment of Pro-1 as a result of HPP binding. (B)  $^1\text{H}$ - $^{15}\text{N}$  HSQC spectra of human MIF in the absence (black) and in the presence (red) of 10 mM HPP. Residues with perturbations greater than the standard deviation for all residues are labeled. (C) Solvent-accessible surface of the human MIF trimer is shown with the monomeric subunits colored blue, yellow and green, and Pro-1 from each subunit colored pink. Residues which were shown to have perturbations  $>1$  standard deviation as a result of HPP binding are colored red. As depicted, these perturbations reveal a binding site that encompasses the N-terminal proline. As seen in the view to the right ( $\sim 150^\circ$  rotation of the left view), much of the protein's surface is unaffected by the binding of HPP.

reduced at  $1 \mu\text{g/ml}$  MIF (Figure 6B). These data indicate that Pro-1 is involved in both the catalytic and biological activity of MIF.

## Discussion

The experiments in this study do not address whether catalysis by MIF is essential for cytokine activity, but the importance of Pro-1 in catalysis and neutrophil activation suggests that an enzymatic reaction may underlie the biological activities of MIF. This suggestion is consistent with previously published results utilizing anti-MIF anti-

bodies. In both *in vivo* and *in vitro* assays anti-MIF antibodies inhibit responses that are not induced by the sole addition of MIF (Bernhagen *et al.*, 1993; Bacher *et al.*, 1996). For example, mice treated with anti-MIF antibodies and a lethal dose of lipopolysaccharide (LPS) survive endotoxemia (Bernhagen *et al.*, 1993). This parallels results obtained with antibodies to other cytokines shown to be involved in sepsis (Tracey *et al.*, 1987; McNamara *et al.*, 1993). However, in contrast to the effects of  $\text{TNF-}\alpha$  (Tracey *et al.*, 1986) and  $\text{IL-1}$  (Okusawa *et al.*, 1988) which induce the sequelae of sepsis in animals, injection of MIF does not cause sepsis. A similar

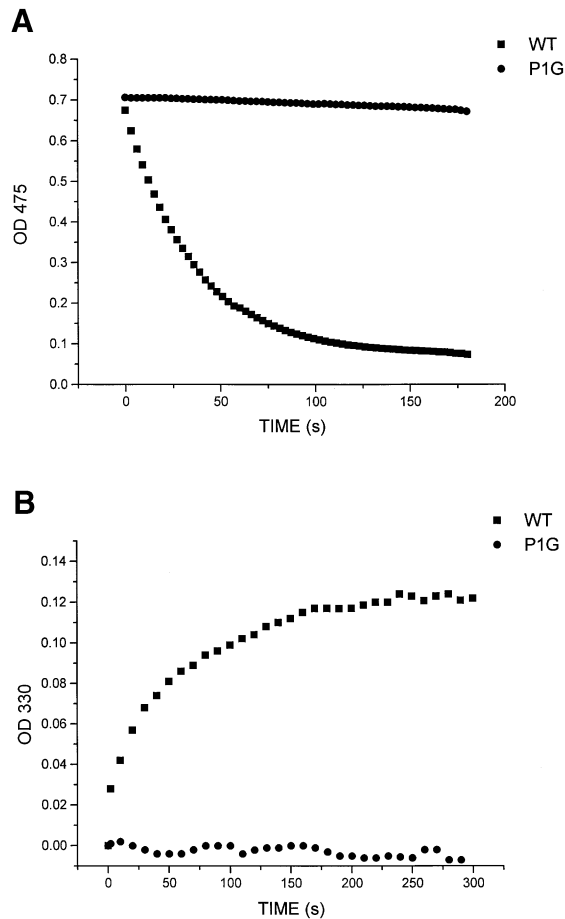


**Fig. 5.** Catalytic activities of wild-type and mutant (P1G) MIF. (A) D-dopachrome tautomerase activity. The absorbance is plotted against the concentration of 2-carboxymethylester-2,3-dihydroindole-5,6-quinone for 100 nM wild-type (■) and P1G (●) MIF. (B) HPP tautomerase activity. The absorbance of enol HPP is plotted against the concentration of keto HPP for 10 nM wild-type (■) and P1G (●) MIF.

paradox involving MIF and its antibodies has been reported in T-cell activation (Bacher *et al.*, 1996). Anti-MIF antibodies inhibit proliferation of T cells, yet MIF does not appear to be a T-cell mitogen. One explanation for these incongruous results is that MIF biological activity requires a cofactor. Antibodies to MIF may therefore inhibit biological activity, but to induce biological activity the cofactor *and* MIF are required. The suggestion that an enzymatic activity underlies MIF biological activity indicates that the essential cofactor may be a substrate for a chemical reaction.

The neutrophil priming activity of MIF is low in comparison with molecules such as lipopolysaccharide, which can prime neutrophils to secrete levels of superoxide 20-fold higher than unprimed cells (Guthrie *et al.*, 1984). The lack of a robust response in the neutrophil priming assay is also consistent with a requirement of a substrate (or cofactor) in MIF biological activity. The decreased priming ability of MIF may be due to the presence of low quantities of the physiological substrate for MIF's catalytic activity under the conditions of the experiment. This possibility can be addressed once the physiological substrate of MIF is identified.

Although MIF can catalyze keto–enol isomerization

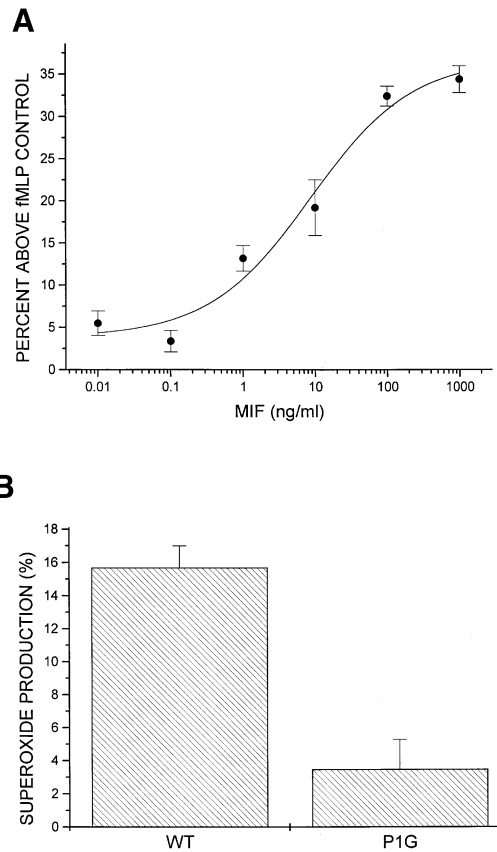


**Fig. 6.** Biological activities of wild-type and mutant (P1G) MIF. (A) Dose–response curve of MIF neutrophil priming activity. Human neutrophils were primed with MIF for 60 min, stimulated with fMLP for 30 min, and the concentrations of superoxide measured. Data are expressed as mean  $\pm$  SEM obtained with neutrophils from four separate donors. (B) Production of superoxide from human neutrophils upon stimulation by wild-type MIF and P1G. Human neutrophils were primed with 1  $\mu$ g/ml MIF or P1G under the same conditions as in (A). The superoxide generated after P1G priming is  $\sim$ 75% lower than with wild-type MIF. Data are expressed as mean  $\pm$  SEM obtained with neutrophils from three separate donors.

reactions of HPP and phenylpyruvate, it is unlikely that these molecules are the natural ligands for MIF. Phenylpyruvate and HPP are generated intracellularly during the biosynthesis of phenylalanine and tyrosine, respectively, and are therefore unable to serve as substrates for extracellular MIF. The serum concentrations of these molecules (Deutsch, 1997) are 1000-fold lower than the  $K_m$  values for MIF, which is also inconsistent with a role as extracellular substrates for MIF. Whether MIF has an intracellular function involving these substrates remains to be investigated.

While the P1G mutant has undetectable D-dopachrome tautomerase and HPP activities under the conditions of the catalytic assays, a low neutrophil priming response is observed. There are at least two potential explanations for this low residual biological activity. First, although the P1G mutant has no measurable catalytic activity using the non-physiological substrates, the mutant protein may have some residual catalytic activity with the unidentified physiological substrate that MIF evolved to utilize. The second possibility is that the P1G mutant may have observable catalytic activity with the non-physiological substrates at the longer timescales required for the neutro-

phil priming assay. Both instances would result in the observed residual neutrophil priming activity of the mutant protein.

It is interesting to note that MIF is not the only protein that possesses both catalytic and cytokine activities. Thrombin (Vu *et al.*, 1991), cyclophilin (Sherry *et al.*, 1992; Xu *et al.*, 1992), FK506 binding protein (Leiva and Lytle, 1992), adenosine deaminase (Kameoka *et al.*, 1993), NAP-2 (Hoogewerf *et al.*, 1995) and neuroleukin (Chaput *et al.*, 1988) are members of an expanding group of proteins with enzymatic and cytokine functions. Of these proteins, the mechanism of cytokine activity of only thrombin has been defined. Thrombin cleaves a proteolytic site at the N-terminal extracellular domain of its G protein-coupled receptor to unmask a tethered ligand that induces self-activation (Vu *et al.*, 1991). Whether other proteins with dual functions utilize their enzymatic active site to induce cytokine activity has not been addressed. The results presented in this study demonstrate that the catalytic site of MIF overlaps with the site responsible for neutrophil activation. The physiological substrate and chemical reaction catalyzed by MIF, and the possible role of this reaction in the pro-inflammatory activities of MIF remain to be determined.

## Materials and methods

### Sequence analysis

The BLAST and ENTREZ programs at the National Center for Biotechnology Information were used to identify MIF homologues. Multiple sequence alignment of these sequences was performed with PILEUP from the GCG package (Devereux *et al.*, 1984).

### Expression and purification of recombinant MIF, P1G mutant MIF and [<sup>15</sup>N]MIF

Recombinant MIF was expressed and purified as previously described (Sun *et al.*, 1996b). The P1G mutant cDNA was generated by PCR using the primer 5'-GCATATACATATGGGCATGTTTCATCGTA-3' that encodes an *NdeI* restriction site (in bold), and a codon for glycine (in italics) instead of a proline after the initiating methionine. The second primer 5'-TTGGATCCTTAGGCGAAGGTGGAGTT-3' annealed to the 3' end of the wild-type cDNA and contained a *BamHI* restriction site (in bold). These restriction sites were used to clone the PCR product into pET-11b for expression and purification of the mutant protein. For biological assays, unlabeled MIF and P1G were made LPS-free as previously published (Bernhagen *et al.*, 1994) and assayed for LPS using the E-Toxate kit (Sigma).

[<sup>15</sup>N]MIF was prepared in minimal media containing 47.9 mM Na<sub>2</sub>HPO<sub>4</sub>, 22 mM KH<sub>2</sub>PO<sub>4</sub>, 8.6 mM NaCl, 7.5 mM (<sup>15</sup>NH<sub>4</sub>)<sub>2</sub>SO<sub>4</sub>, 22.2 mM glucose, 1.99 mM MgSO<sub>4</sub>·7H<sub>2</sub>O, 100 μM CaCl<sub>2</sub>·2H<sub>2</sub>O, 26 μM FeCl<sub>3</sub>·6H<sub>2</sub>O, 60 μM thiamin hydrochloride, 82.5 μM thymidine, <sup>15</sup>N-labeled Celtone (Martek, Columbia, MD), 2.5 μM biotin and 100 μg/ml ampicillin. Briefly, an overnight culture of pET-11b MIF in BL21(DE3) cells was added to labeled minimal media in a baffled flask and grown at 37°C until the culture reached an OD<sub>600</sub> 0.7–1.0. IPTG was added to a final concentration of 1 mM and the cells were induced overnight.

### NMR studies

All NMR measurements were made on either a DMX500 or DMX600 NMR spectrometer operating at 500.152 and 600.144 MHz, respectively. One-dimensional <sup>15</sup>N spectra were collected on 2.3 mM samples of [<sup>15</sup>N]MIF in 20 mM phosphate, pH 6.8 using a Bruker 5 mM broadband probe with the following acquisition parameters: spectrometer frequency, 50.684 MHz; spectral width, 11 468 Hz; acquisition time, 714 ms; relaxation delay, 100 ms; total transients, 25–90 k; temperature, 295°K. Sample pH adjustments were achieved using 0.5–2 μl additions of 1.2–1.3 M NaOH or HCl. Two-dimensional <sup>1</sup>H-<sup>15</sup>N-HSQC spectra were collected on a 1 mM sample of [<sup>15</sup>N]MIF in 20 mM phosphate, pH 6.8 using a Bruker 5 mm triple resonance probe with three-axis gradients.

Chemical shift assignments for human MIF were published previously (Muhlhahn *et al.*, 1996). HPP (Sigma) was dissolved in 1 M ammonium hydroxide and the pH adjusted with 1 M HCl prior to addition to [<sup>15</sup>N]MIF. Acquisition parameters for <sup>1</sup>H-<sup>15</sup>N HSQC spectra were as follows: spectrometer frequency, 600.139 MHz; spectral width, 5388 Hz; acquisition time, 95 ms; recycle delay, 1 s; transients per-block, 32; complex blocks, 128; temperature, 298°K. To facilitate sample locking, 5% D<sub>2</sub>O was added to all samples.

### X-ray studies

Crystals of MIF in space group P3<sub>1</sub>21 with unit cell dimensions  $a = b = 96.70 \text{ \AA}$ ,  $c = 106.14 \text{ \AA}$  were obtained as described previously (Sun *et al.*, 1996b). X-ray data were collected at room temperature as 2° frames on a Rigaku R-Axis IIC image-plate detector and a Rigaku RU200 rotating anode generator equipped with mirror optics. The data collected to a resolution of 1.9 Å were processed using BIOTEX (Molecular Structure Corp., Woodlands, TX) and consisted of 40 317 reflections from a total of 130 276 observations ( $F^2/\sigma(F^2) \geq 1.0$ ) with an  $R_{\text{merge}}$  of 8.9%. Simulated annealing was first used to refine the 2.6 Å model to an R-factor of 23.4% for data from 5.0 to 2.2 Å. Restrained B-factor refinement followed by several rounds of positional refinement and rebuilding resulted in an R-factor of 23% for data from 5.0 to 1.9 Å. Simulated annealing omit maps and PROCHECK (Laskowski *et al.*, 1993) were used to analyze the model. Manual adjustments, including the addition of water molecules, were made as necessary. The final model was subjected to individual B-factor least-squares refinement. The free R-factor calculation (Brunger, 1992) was included throughout to monitor the refinement. The final structure of trigonal MIF has a free R-factor of 26.4% and an overall R-factor of 20.9% at 1.9 Å resolution with r.m.s. deviations of 0.009 Å and 1.6° for bond lengths and bond angles, respectively.

For calculation of the electrostatic potential, arginine, aspartic acid, glutamic acid and lysine side chains were assigned unit charges, histidine side chains were assigned a charge of +0.5, and the terminal amine and carboxylate of the polypeptide were left uncharged. The interior and exterior dielectric constants were 2 and 80, respectively. All calculations were carried out using DELPHI (MSI, San Diego, CA).

### Biological and catalytic activities

Neutrophils were prepared from freshly drawn blood anticoagulated with heparin. Blood was diluted with physiological saline for irrigation, layered over lymphocyte separation medium (Organon Teknica), and subjected to centrifugation at 400 g for 30 min. The supernatant containing lymphocytes and serum was aspirated and the red blood cell pellet diluted with an equal volume of 3% dextran and allowed to separate until there was a defined interface. The supernatant containing neutrophils was collected, washed with supplemented Hanks balanced salt solution (HBSS) containing 0.2% dextrose, Ca<sup>2+</sup> and Mg<sup>2+</sup>, and residual red blood cells lysed by hypotonic lysis. Neutrophils were pelleted by centrifugation, resuspended in supplemented HBSS with 1% human serum added and used immediately for experiments.

Neutrophils were primed by incubating  $2.5 \times 10^6$  cells for 1 h at 37°C in supplemented HBSS/1% serum containing varying concentrations of recombinant MIF. LPS contamination for both wild-type MIF and P1G was <0.15 pg/μg of protein. Neutrophils were pelleted by centrifugation, resuspended in 120 μM cytochrome *c* in supplemented HBSS, treated with 10<sup>-5</sup> M fMLP, and incubated at 37°C for 30 min. Superoxide-specific reduction of cytochrome *c* was determined spectrophotometrically using cells incubated with or without 50 μg/ml superoxide dismutase.

For D-dopachrome tautomerase assays, L-dopachrome methyl ester was prepared by mixing 4 mM L-3,4-dihydroxyphenylalanine methyl ester with 8 mM sodium periodate for 5 min at room temperature and then placed directly on ice for 20 min before use. Activity was determined at 25°C by adding dopachrome methyl ester to a cuvette containing 100 nM MIF or P1G in 25 mM potassium phosphate buffer pH 6, 0.5 mM EDTA and measuring the decrease in absorbance at 475 nm on a Hewlett Packard 8452 diode array spectrophotometer.

For HPP tautomerase assays, HPP was dissolved in 50 mM ammonium acetate pH 6.0, allowed to equilibrate at room temperature overnight, and stored at 4°C. Activity was determined at 25°C by adding HPP to a quartz cuvette containing 10 nM MIF or P1G, 0.435 M boric acid, pH 6.2, and measuring the increase in absorbance at 330 nm spectrophotometrically.

## Acknowledgements

We thank Professor William Lipscomb (Harvard University) for alerting us to the similarity between MIF and chorismate mutase, Alan Scott

(Johns Hopkins University) for the parasitic sequences prior to publication, Hans Rorsman (University of Lund) for information on the phenylpyruvate tautomerase activity prior to publication, and Joe Vaccaro (Yale University), Richard Johnston (Yale University) and Christian Whitman (University of Texas) for helpful discussions.

## References

- Bacher, M., Metz, C., Calandra, T., Mayer, K., Chesney, J., Lohoff, M., Gemsa, D., Donnelly, T. and Bucala, R. (1996) An essential role for MIF in T cell activation. *Proc. Natl Acad. Sci. USA*, **93**, 7849–7854.
- Bernhagen, J., Calandra, T., Mitchell, R.A., Martin, S.B., Tracey, K.J., Voelter, W., Manogue, K.R., Cerami, A. and Bucala, R. (1993) MIF is a pituitary-derived cytokine that potentiates lethal endotoxaemia. *Nature*, **365**, 756–759.
- Bernhagen, J., Mitchell, R.A., Calandra, T., Voelter, W., Cerami, A. and Bucala, R. (1994) Purification, bioactivity, and secondary structure analysis of mouse and human macrophage migration factor (MIF). *Biochemistry*, **33**, 14144–14155.
- Bernhagen, J., Bacher, M., Calandra, T., Metz, C., Doty, S.B., Donnelly, T. and Bucala, R. (1996) An essential role for macrophage migration inhibitory factor in the tuberculin delayed-type hypersensitivity reaction. *J. Exp. Med.*, **183**, 277–282.
- Bloom, B.R. and Bennett, B. (1966) Mechanism of a reaction *in vitro* associated with delayed-type hypersensitivity. *Science*, **153**, 80–82.
- Brunger, A.T. (1992) Free R-value: a novel statistical quantity for assessing the accuracy of crystal structures. *Nature*, **355**, 472–475.
- Calandra, T., Bernhagen, J., Metz, C.N., Spiegel, L., Bacher, M., Donnelly, T., Cerami, A. and Bucala, R. (1995) MIF as a glucocorticoid-induced modulator of cytokine production. *Nature*, **377**, 68–71.
- Chaput, M., Claes, V., Portetelle, D., Cludts, I., Cravador, A., Burny, A., Gras, H. and Tartar, A. (1988) The neurotropic factor neuroleukin is 90% homologous with phosphohexose isomerase. *Nature*, **332**, 454–455.
- Chook, Y.M., Gray, J.V., Ke, H. and Lipscomb, W.N. (1994) The monofunctional chorismate mutase from *Bacillus subtilis*. Structure determination of chorismate mutase and its complexes with a transition state analog and prephenate, and its implications for the mechanism of the enzymatic reaction. *J. Mol. Biol.*, **240**, 476–500.
- David, J.R. (1966) Delayed hypersensitivity *in vitro*: its mediation by cell-free substances formed by lymphoid cell-antigen interaction. *Proc. Natl Acad. Sci. USA*, **56**, 72–77.
- Deusch, J. (1997) Determination of *p*-hydroxyphenylpyruvate, *p*-hydroxyphenyllactate and tyrosine in normal human plasma by gas chromatography-mass spectrometry isotope-dilutions assay. *J. Chromatogr.*, **B690**, 1–6.
- Devereux, J., Haerberli, P. and Smithies, O. (1984) A comprehensive set of sequence analysis programs for the VAX. *Nucleic Acids Res.*, **12**, 387–395.
- Galat, A., Riviere, S. and Bouet, F. (1993) Purification of macrophage migration inhibitory factor from bovine brain cytosol. *FEBS Lett.*, **319**, 233–236.
- Guthrie, L., McPhail, L., Henson, P. and Johnston, R. (1984) Priming of neutrophils for enhanced release of oxygen metabolites by bacterial lipopolysaccharide. *J. Exp. Med.*, **160**, 1656–1671.
- Hajjipour, G., Johnson, W.H., Dauben, P.D., Stolowich, N.J. and Whitman, C.P. (1993) Chemical and enzymatic ketonization of 5-(carboxymethyl)-2-hydroxy-muconate. *J. Am. Chem. Soc.*, **115**, 3533–3542.
- Hoogewerf, A., Leone, J., Reardon, I., Howe, J., Asa, D., Henrikson, R. and Ledbetter, S. (1995) CXC chemokines connective tissue activating peptide-III and neutrophil activating peptide-2 are heparin/heparan sulfate-degrading enzymes. *J. Biol. Chem.*, **270**, 3268–3277.
- Kameoka, J., Tanaka, T., Nojima, Y., Schlossman, S.F. and Morimoto, C. (1993) Direct association of adenosine deaminase with a T cell activation antigen, CD26. *Science*, **261**, 466–469.
- Kato, Y., Muto, T., Tomura, T., Tsumura, H., Watarai, H., Mikayama, T., Ishizaka, K. and Kuroki, R. (1996) The crystal structure of human glycosylation-inhibition factor is a trimeric barrel with three 6-stranded beta sheets. *Proc. Natl Acad. Sci. USA*, **93**, 3007–3010.
- Laskowski, R.A., MacArthur, M.W., Moss, D. and Thornton, J.M. (1993) Procheck: a program to check the stereochemical quality of protein structure. *J. Appl. Crystallogr.*, **26**, 283–291.
- Leiva, M.C. and Lytle, C.R. (1992) Leukocyte chemotactic activity of FKBP and inhibition of FK506. *Biochem. Biophys. Res. Commun.*, **186**, 1178–1183.
- McNamara, M.J., Norton, J.A., Nauta, R.J. and Alexander, H.R. (1993) Interleukin-1 receptor antibody protection and treatment against lethal endotoxaemia in mice. *J. Surg. Res.*, **54**, 316–321.
- Mikayama, T. *et al.* (1993) Molecular cloning and functional expression of a cDNA encoding glycosylation-inhibiting factor. *Proc. Natl Acad. Sci. USA*, **90**, 10056–10060.
- Muhlhahn, P., Bernhagen, J., Czisch, M., Georgescu, J., Renner, C., Ross, A., Bucala, R. and Holak, T.A. (1996) NMR characterization of structure, backbone dynamics, and glutathione binding of the human macrophage migration inhibitory factor (MIF). *Protein Sci.*, **5**, 2095–2103.
- Okusawa, S., Gelfand, J.A., Ikejima, T., Connolly, R.J. and Dinarello, C.A. (1988) Interleukin-1 induces a shock-like state in rabbits. Synergism with tumor necrosis factor and the effect of cyclooxygenase inhibition. *J. Clin. Invest.*, **81**, 1162–1172.
- Rosengren, E., Bucala, R., Arnan, P., Jacobsson, L., Odh, G., Metz, C.N. and Rorsman, H. (1996) The immunoregulatory macrophage migration inhibitory factor (MIF) catalyzes a tautomerization reaction. *Mol. Med.*, **2**, 143–149.
- Rosengren, E., Aman, P., Thelin, S., Hansson, C., Ahlfors, S., Bjork, P., Jacobsson, L. and Rorsman, H. (1997) The macrophage migration inhibitory factor MIF is a phenylpyruvate tautomerase. *FEBS Lett.*, **417**, 85–88.
- Sherry, B., Yarlett, N., Strupp, A. and Cerami, A. (1992) Identification of cyclophilin as a proinflammatory secretory product of lipopolysaccharide-activated macrophages. *Proc. Natl Acad. Sci. USA*, **89**, 3511–3515.
- Stivers, J.T., Abeygunawardana, C. and Mildvan, A.S. (1996) 4-oxalocrotonate tautomerase: pH dependence of catalysis and pK<sub>a</sub> values of active site residues. *Biochemistry*, **35**, 814–823.
- Subramanya, H.S., Roper, D.I., Dauter, D., Dodson, E.J., Davies, G.J., Wilson, K.S. and Wigley, D.B. (1996) Enzymatic ketonization of 2-hydroxy-muconate: specificity and mechanism investigated by the crystal structures of two isomerases. *Biochemistry*, **35**, 792–802.
- Sun, H.W., Bernhagen, J., Bucala, R. and Lolis, E. (1996a) Crystal structure at 2.6 Angstrom resolution of human macrophage migration inhibitory factor. *Proc. Natl Acad. Sci. USA*, **93**, 5191–5196.
- Sun, H.W., Swope, M., Cinquina, C., Bedarkar, S., Bernhagen, J., Bucala, R. and Lolis, E. (1996b) Subunit structure of human migration inhibitory factor: evidence for a trimer. *Protein Eng.*, **9**, 631–635.
- Suzuki, M., Sugimoto, H., Nakagawa, A., Tanaka, I., Nishihara, J. and Sakai, M. (1996) Crystal structure of the macrophage migration inhibitory factor from rat liver. *Nature Struct. Biol.*, **3**, 259–266.
- Tracey, K.J. *et al.* (1986) Shock and tissue injury induced by recombinant human cachectin. *Science*, **234**, 470–474.
- Tracey, K.J., Fong, Y., Hesse, D.G., Manogue, K.R., Lee, A.T., Kuo, G.C., Lowry, S.F. and Cerami, A. (1987) Anti-cachectin/TNF monoclonal antibodies prevent septic shock during lethal bacteraemia. *Nature*, **330**, 662–664.
- Vu, T., Wheaton, V., Hung, D., Charo, I. and Coughlin, S. (1991) Domains specifying thrombin-receptor interaction. *Nature*, **353**, 674–677.
- Whitman, C.P., Aird, B.A., Gillespie, W.R. and Stolowich, N.J. (1991) Chemical and enzymatic ketonization of 2-hydroxy-muconate, a conjugated enol. *J. Am. Chem. Soc.*, **113**, 3154–3162.
- Xu, Q., Leiva, M.C., Fischkoff, S.A., Handschumacher, R.E. and Lytle, C.R. (1992) Leukocyte chemotactic activity of cyclophilin. *J. Biol. Chem.*, **267**, 11968–11971.

Received January 16, 1998; revised and accepted May 7, 1998